

Discovery of 2-pyrimidyl-5-amidothiophenes as potent inhibitors for AKT: Synthesis and SAR studies

Xiaodong Lin,* Jeremy M. Murray, Alice C. Rico, Michael X. Wang, Daniel T. Chu, Yasheen Zhou, Merci Del Rosario, Susan Kaufman, Sylvia Ma, Eric Fang, Kenneth Crawford and A. B. Jefferson

Small Molecule Drug Discovery, Biopharma Research, Chiron Corporation, 4560 Horton Street, Emeryville, CA, USA

Received 14 April 2006; revised 25 May 2006; accepted 30 May 2006

Available online 9 June 2006

Abstract—A series of 2-pyrimidyl-5-amidothiophenes has been synthesized and evaluated for AKT inhibition. SAR studies resulted in potent inhibitors of AKT with IC_{50} values as low as single digit nanomolar as represented by compound **2aa**. Compound **2aa** showed cellular activity including antiproliferation and downstream target modulation. Selectivity profile is described. A co-crystal of **2aa** with PKA is determined and discussed.

© 2006 Elsevier Ltd. All rights reserved.

AKT is a serine/threonine kinase that plays a central role in diverse cellular functions including cell growth and proliferation, metabolism, and apoptosis. A number of growth factors and cytokines activate phosphatidylinositol-3 kinase (PI3K), which then phosphorylates membrane phosphatidylinositols. The most highly phosphorylated of these, $PI(3,4,5)P_3$, essentially serves as a tethered ligand, directing the membrane localization and activation of a number of cellular enzymes including PDK1 and AKT. Full activation of AKT requires phosphorylation by PDK1 and an undefined PDK2. AKT, in turn, phosphorylates a growing list of substrates including GSK3, FOXO transcription factors, MDM2, TSC1/2, and BAD.^{1,2}

Not surprisingly, given the many cellular functions regulated by AKT signaling, tumor cells have selected for multiple circumventions of the normal checks on this pathway.³ PTEN, a phosphatidylinositol phosphatase that negatively regulates this pathway, is one of the most frequently inactivated genes in tumors. Several receptor tyrosine kinases such as EGFR and Her2 that signal through the AKT pathway are overexpressed in cancer,

and PI3K has also been shown to have activating mutations in tumors. Finally, each of the three AKT family members (AKT1, AKT2, and AKT3)^{4–7} has been shown to be amplified or overexpressed in at least one cancer type. Thus, there are a number of patient populations who might benefit from inhibition of signaling through this pathway at the level of AKT.

Multiple approaches are being taken to target AKT.^{3,4,8,9} AKT binds to $PI(3,4,5)P_3$ via a pleckstrin homology (PH) domain suggesting the possibility of inhibiting AKT by interfering with this association. Another strategy takes advantage of the sequence diversity in the hinge region between the PH domain and kinase domains of AKT1,2,3 to create isoform-selective allosteric inhibitors. But by far the most highly explored strategy is to target AKT's kinase domain with ATP-competitive inhibitors. While this strategy has a high likelihood of generating potent inhibitors, it presents the challenge of achieving selectivity, since the ATP-binding site of AKT has high homology to other AGC group kinases, particularly PKA.¹⁰ Small molecule AKT inhibitors have been reported in recent literature including ATP-competitive inhibitors^{11–14} as well as allosteric inhibitors.¹⁵

Compound **1** (Fig. 1) was identified as an AKT3 inhibitor via high throughput screening of our compound collection. It is an ATP-competitive inhibitor with an IC_{50}

Keywords: Protein kinase B/AKT; kinase inhibitor; Substituted pyrimidine; Cancer.

* Corresponding author. Tel.: +1 510 923 7752; fax: +1 510 923 3360; e-mail: xiaodong_lin@chiron.com

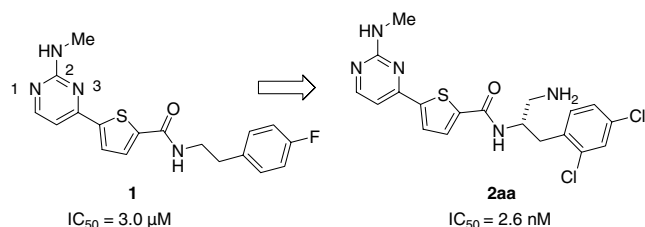
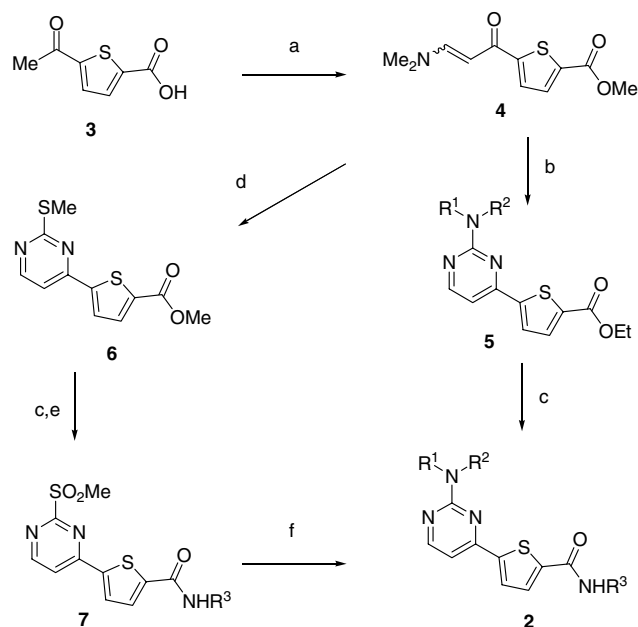


Figure 1. From a low micromolar hit **1** to a potent inhibitor **2aa**.

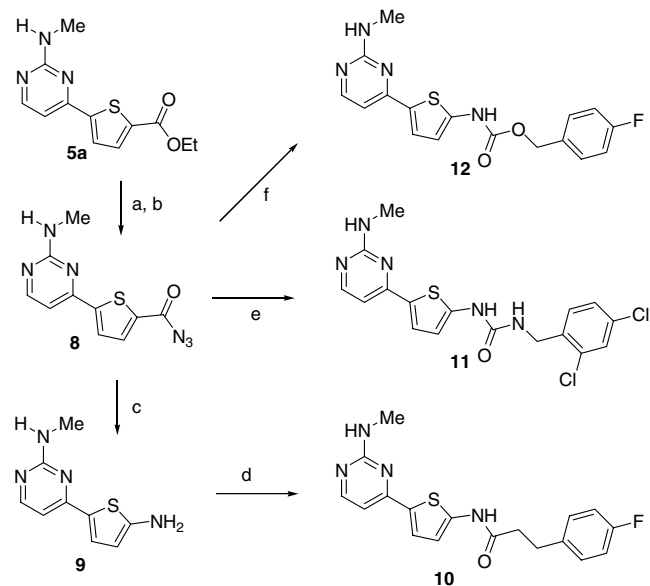
of 3.0 μM against AKT3. We report herein the structural modifications of this compound, which led to a series of novel and potent AKT inhibitors exemplified by compound **2aa**.

Synthesis of analogs of 2-pyrimidyl-5-amidothiophene is depicted in **Scheme 1**. Starting with 5-acetylthiophene-2-carboxylic acid **3**, the aminopyrimidine ring was formed by a two-step sequence to give ethyl ester **5**. The subsequent amide bond formation with various amines then yielded analogs **2**. Alternatively, 2-methylthiopyrimidine **6** was built from vinylogous amide **4** and *S*-methylisothioureia. Amide bond formation and oxidation then gave sulfone **7**. Finally S_NAr reaction with amines gave analogs **2**. These two sequences enabled efficient variation of amide position and 2-amino position of the pyrimidine.

The amide function in **1** can be modified into reverse amide unit, urea and carbamate, using **5a** as the intermediate. As shown in **Scheme 2**, intermediate acylazide **8**



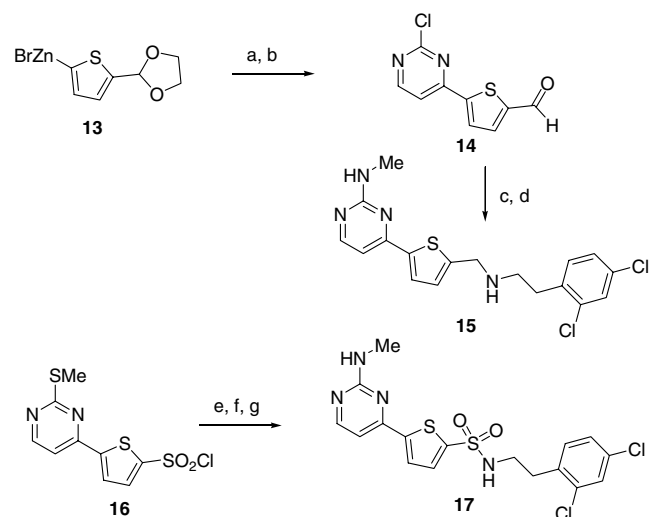
Scheme 1. Reagents and conditions: (a) *N,N*-dimethylformamide dimethyl acetal, toluene, 110 °C, 16 h, 91%; (b) 1-methylguanidine hydrochloride or guanidine hydrochloride, NaOEt, EtOH, 70 °C, 40 h, 45–58%; (c) substituted phenethylamine R³NH₂, NaOMe, MeOH, 44 h, 7–55%; (d) *S*-methylisothioureia hemisulfate, pyridine, H₂O, 100 °C, 68 h, 69%; (e) *m*-CPBA, DCM, rt, 100%; (f) amines R¹R²NH, 1,4-dioxane, 110 °C, 3–16 h, 40–55%.



Scheme 2. Reagents and conditions: (a) hydrazine, MeOH, 70 °C, 16 h, 87%; (b) 0.6 M HCl_(aq), NaNO₂, HOAc, 0 °C, 30 min, 91%; (c) 1.5 M HCl_(aq), 100 °C, 16 h, 30%; (d) 3-(4-fluorophenyl)propionic acid, CDI, THF, 50 °C, 30 min; then **9**, 2 h, 50 °C, 30%; (e) xylenes, 120 °C, 25 min; then 2,4-dichlorobenzylamine, 120 °C, 30 min, 12%; (f) xylenes, 120 °C, 25 min; then 4-fluorobenzylalcohol, xylenes, 120 °C, 45 min, 11%.

was formed by treating **5a** with hydrazine followed by diazotization. Subsequent Curtius rearrangement using 2,4-dichlorobenzylamine and 4-fluorobenzyl alcohol yielded urea **11** and carbamate **12**, respectively. Curtius rearrangement using HCl gave aminothiophene **9**, which was converted to desired reverse amide **10**.

Scheme 3 summarizes the synthesis of **15** and **17**. Analog **15** was prepared using commercially available thiophe-



Scheme 3. Reagents and conditions: (a) 2,4-dichloropyrimidine, (PPh₃)₄Pd(0), THF, 70 °C, 16 h; (b) 1.2 M HCl_(aq), acetone, 16 h, rt; (c) 2,4-dichlorophenethylamine, toluene, 110 °C, 4 h, removed volatiles, MeOH, NaBH₄, 2 h, rt, 54%; (d) MeNH₂, THF, 75 °C, 16 h, 47%; (e) 2,4-dichlorophenethylamine, TEA, DCM, 3 h, rt; (f) *m*-CPBA, 16 h, 100%; (g) MeNH₂, THF, 75 °C, 16 h, 25%.

nyl zinc bromide **13**. Negishi cross-coupling with 2,4-dichloropyrimidine followed by hydrolysis gave intermediate **14**. Reductive amination and S_NAr with methylamine yielded desired secondary amine analog. Sulfonamide analog **17** was synthesized using commercially available starting material **16** via a straightforward three-step sequence.

We started SAR studies by changing the fluorophenyl ring in **1**, as well as evaluating the tether length between the phenyl ring and the amide nitrogen. As summarized in Table 1, the tether length is very important to potency (**1**, **2a–c**). The optimal length appears to be two carbon atoms (**1**). Using commercially available substituted phenethylamines, we found that both the position and the nature of substituents on the phenyl ring are crucial to potency. Although it is clear that *para*-halogens are beneficial (**2g** vs **2d**), a chloro group (**2g**) is only marginally superior to fluoro (**1**) and bromo (**2h**) groups. Substituents other than halogens such as methyl, methoxyl, and aminosulfonyl are detrimental to the activity (**2i–k**). *para*-Pyridyl is also detrimental (**2l**). It was also observed that *ortho*- and *meta*-chloro groups are less potent than corresponding *para*-analog (**2f**, **2e** vs **2g**). Among several dihalogen substitutions, 2,4-dichloro appears the best (**2m**).

At this point, we decided to fix the right-hand side as 2,4-dichlorophenethyl group in order to evaluate the effect of substitution on 2-amino group of the pyrimidine ring. Based upon a homology model, we have postulated (later confirmed by X-ray co-crystal structure, *vide infra*) that the aminopyrimidine portion of molecule **1** interacts with the hinge domain of the kinase. It is

important for potency to maintain N1 and 2-NH (Fig. 1) as H-bond acceptor and donor, respectively. As shown in Table 1, when the 2-amino group is bis-substituted (**2q**), the potency against AKT3 is completely eliminated. Replacing the methyl group on the 2-amino position with groups bigger than ethyl (**2o** vs **2p**) leads to much less potent inhibitors, indicating restricted protein space in this region. Other substituents all proved to be detrimental to the potency. Throughout our study, we have observed that 2-amino and 2-amino-methyl substituent gave similar potency as exemplified by **2n** and **2m**.

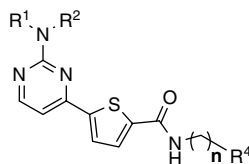
Next, we decided to probe the effect of the amide group in **1**. As shown in Table 2, changing the amide group to its reversed amide analog **10** or urea analog **11** does not affect binding potency. Changing the amide to carbamate **12** and less constrained amine analog **15** leads to slightly decreased potency. However, sulfonamide analog **17** lost potency completely. These data suggest that the amide bond is important sterically to place the substituted phenyl group in a proper orientation for potency. In contrast to *s-trans* conformation of an

Table 2. Activity of AKT inhibitors^a

Compound	IC ₅₀ (nM, AKT3)
1	3000
10	2300
11	2100
12	7400
15	5200
17	>25,000

^a AKT3 as assayed at 0.2 μM ATP in the presence of MnCl₂.

Table 1. Activity of AKT inhibitors^a



Compound	R ¹	R ²	R ⁴	n	IC ₅₀ (nM, AKT3)
1	H	Me	4-Fluorophenyl	2	3000
2a	H	Me	4-Fluorophenyl	1	4700
2b	H	Me	4-Fluorophenyl	0	>25,000
2c	H	Me	4-Fluorophenyl	3	18,000
2d	H	Me	Phenyl	2	5000
2e	H	Me	3-Chlorophenyl	2	5400
2f	H	Me	2-Chlorophenyl	2	2900
2g	H	Me	4-Chlorophenyl	2	1100
2h	H	Me	4-Bromophenyl	2	2600
2i	H	Me	4-Methylphenyl	2	>25,000
2j	H	Me	4-Methoxyphenyl	2	>25,000
2k	H	Me	4-Sulfamoylphenyl	2	19,000
2l	H	Me	4-Pyridyl	2	>25,000
2m	H	Me	2,4-Dichlorophenyl	2	990
2n	H	H	2,4-Dichlorophenyl	2	610
2o	H	Et	2,4-Dichlorophenyl	2	1500
2p	H	Pr	2,4-Dichlorophenyl	2	>25,000
2q	Me	Me	2,4-Dichlorophenyl	2	>25,000

^a AKT3 as assayed at 0.2 μM ATP in the presence of MnCl₂.

amide bond, sulfonamides prefer *s-cis* ground state conformation. Therefore, the phenyl group in the sulfonamide analog is no longer projected with the right conformation for potency.

Substitution on the two-carbon chain between the phenyl ring and amide nitrogen of **1** proved to be very important for AKT3 potency. Table 3 summarizes the effect of carbon chain substitution. It was clear that the substituent R⁶ at the benzylic position (when R⁷ is phenyl or substituted phenyl) can tolerate small alkyl groups (**2r** and **2s**) and basic amino group (**2u**). The bigger phenyl group is not tolerated as R⁶ (**2t**). Small groups such as methyl (**2v**) and methyl ester (**2w**) are tolerated at homobenzylic position R⁵ (when R⁷ is substituted phenyl). Polar group hydroxymethyl (**2x**) improved potency about 4-fold (compared to **2m**). To our excitement, basic aminomethyl group boosted potency to 4.8 nM (**2y**). The *S*-enantiomer **2aa** proved to have the optimal configuration (compared to *R*-enantiomer **2z**) for the binding. Substitutions on the primary amine (**2bb**) as well as moving the amino group further away (**2cc**) turned out to be less potent. Removal of the benzylic group resulted in more than 500-fold potency loss (**2dd** vs **2aa** and **2ee** vs **2bb**). Therefore, both substituted phenyl ring and a properly positioned primary amine are crucial for the potency.

The co-crystal structure of **2aa** in complex with PKA was determined by X-ray crystallography (Fig. 2, 3).¹⁶ PKA has previously been used as a surrogate for AKT in structure-based drug design.^{12–14} The co-crystal structure of **2aa** with PKA rationalizes much of the SAR. The 2-aminopyrimidyl group binds to the hinge via hydrogen bond interactions between the 2-amino group and the backbone carbonyl group of Glu121, and the

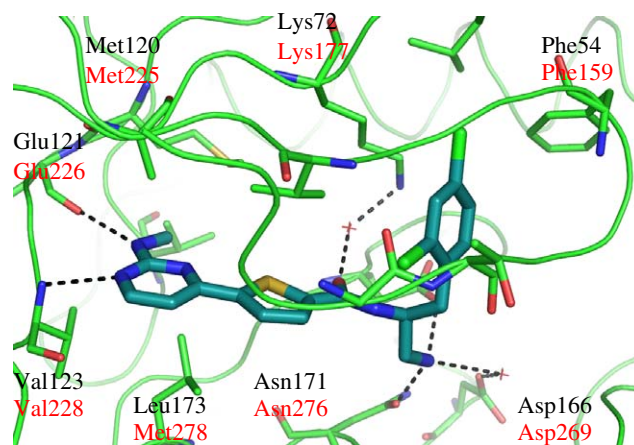
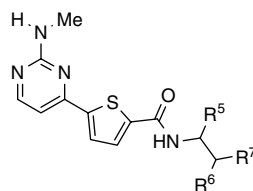


Figure 2. X-ray crystal structure of **2aa** in complex with PKA in the active site with key interactions highlighted. The amino acids highlighted in black are from PKA and red are from AKT3.

pyrimidine N1 and the backbone nitrogen of Val123. The effects of the substitutions at the 2-amino position of the pyrimidine are due to the close packing of residues around the methyl group which is 3.5 Å from the C ϵ of Met120. The residues within 4 Å of the pyrimidine moiety are mainly hydrophobic in nature (Val57, Ala70, Val104, Met120, and Leu173), and the thiophene moiety is sandwiched above and below the plane by the side-chains of Val57 and Leu173. The oxygen atom of the central amide group makes a water-mediated interaction with the catalytic lysine (Lys72) indicating that the exact placement of the hydrogen bonding atoms in this portion of the molecule is less important than the role that this portion plays in ensuring the correct orientation for the substituted phenyl group.

Table 3. Activity of AKT inhibitors^a



Compound	R ⁵	R ⁶	R ⁷	IC ₅₀ (nM, AKT3)
2r	H	Me	2,4-Dichlorophenyl	660
2s	H	Et	2,4-Dichlorophenyl	1000
2t	H	Phenyl	Phenyl	>25,000
2u	H	-NH ₂ (<i>S</i>)	Phenyl	2800
2v	-Me (<i>R</i>)	H	2,4-Dichlorophenyl	820
2w	-CO ₂ Me (<i>S</i>)	H	2,4-Dichlorophenyl	2400
2x	-CH ₂ OH (<i>S</i>)	H	2,4-Dichlorophenyl	280
2y	-CH ₂ NH ₂	H	2,4-Dichlorophenyl	4.8
2z	-CH ₂ NH ₂ (<i>R</i>)	H	2,4-Dichlorophenyl	240
2aa	-CH ₂ NH ₂ (<i>S</i>)	H	2,4-Dichlorophenyl	2.6
2bb	-CH ₂ NMe ₂ (<i>S</i>)	H	2,4-Dichlorophenyl	11
2cc	-CH ₂ CH ₂ NH ₂ (<i>S</i>)	H	2,4-Dichlorophenyl	27
2dd	H	H	NH ₂	1300
2ee	H	H	NMe ₂	7000

^a AKT3 as assayed at 0.2 μM ATP in the presence of MnCl₂.

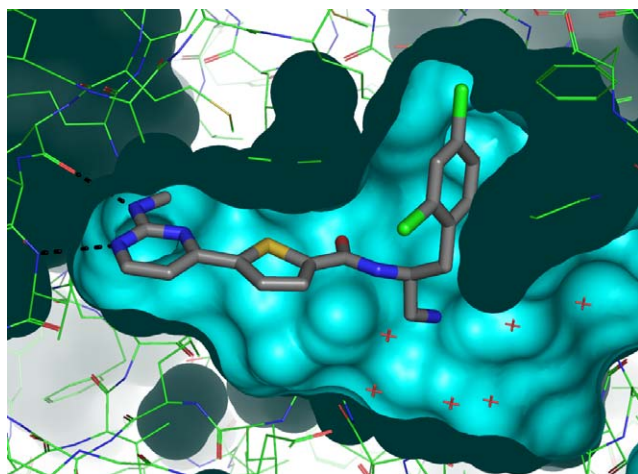


Figure 3. X-ray crystal structure of compound **2aa** bound to the ATP binding site of PKA.

The primary amino group of the aminomethyl makes important interactions as it projects into one of the Mg^{2+} binding pockets of PKA, and it makes two direct hydrogen bond interactions with protein sidechains, one with Asn171 and the other with Asp184 from the DFG. There is also a water-mediated interaction with Asp166. Comparison of **2z** and **2aa** in Table 3 shows that the precise positioning of this group has a 100-fold effect on potency. The tip of the Gly-rich loop clamps down around the disubstituted phenyl moiety, with Phe54 swinging down to exclude bulk solvent from the active site (Fig. 3). The *para*-Cl group points up into a predominantly hydrophobic environment created by the sidechain methylene groups of Phe54, Val57, Leu74, and Lys72. The *ortho*-Cl group projects into a space between Val57 and the mainchain carbon atoms of Gly50 and Thr51.

The selectivity and cellular activity of **2aa** are listed in Table 4. The compound has some degree of selectivity

Table 4. Selectivity profile and cellular activity of AKT inhibitor **2aa**

Test	Name	2aa (nM)	Staurosporin (nM)
Kinases ^a	AKT1	6	11
	AKT2	23	9
	AKT3	3	5
	PKA	0.1	0.9
	PKCa	66	1
	Kit	110	>1
	Met	1100	130
	EGFR	>10,000	19
	CaMK2 α	8000	>1
	ERK1	400	4900
Cellular activity	DOV13 ^b	1000	ND
	GSK3 S9P ^c	320	ND
	PRAS40 T246P ^c	160	ND
	S6RP S235/236P ^c	370	ND

^a All kinase IC_{50} s were assayed at or below K_m for ATP.

^b Cell proliferation EC_{50} determined by Promega Cell TiterGlo.

^c Cell phosphorylation EC_{50} determined by scanned Western blot in DOV13 ovarian carcinoma cells.

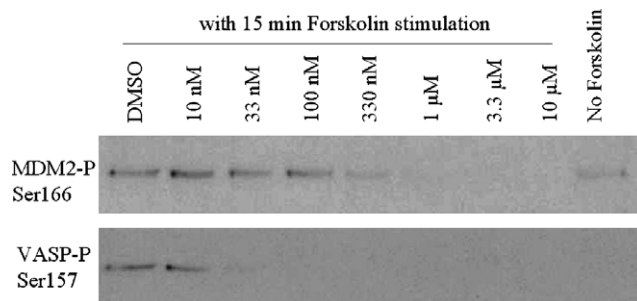


Figure 4. Compound **2aa** inhibits PKA more potently than AKT in UACC903 cells. Cells were treated with **2aa** for 45 min prior to stimulation with 7 μ M forskolin for 15 min. Cell lysates were Western blotted for phosphorylation of VASP by PKA (cell signaling #3111) or MDM2 by AKT (cell signaling #3521).

against other kinases with the exception of PKA, and it shows good inhibition of proliferation and AKT target phosphorylation in the ovarian carcinoma cell line, DOV13.

While this compound appears to inhibit PKA at least 30x more potently than AKT, we sought to confirm this in vitro potency differential in a cell line in which both kinases were active concurrently. Thus, we pre-incubated UACC903 melanoma cells with various concentrations of compound **2aa** before stimulation with the PKA activator, forskolin, for 15 min prior to cell lysis (Fig. 4). PKA activity could be monitored through its phosphorylation of VASP on Ser157 in response to forskolin stimulation, while AKT activity was monitored by basal MDM2 phosphorylation on Ser166. Compound **2aa** inhibited cellular PKA activity at between 10 and 33 nM concentration, while AKT activity was inhibited at 330 nM to 1 μ M of **2aa**. Thus, the apparent ratio of inhibition of the two kinases observed in vitro was confirmed in cells.

In summary, we have developed a series of 2-pyrimidyl-5-amidothiophene as potent AKT inhibitors. Compounds in the series showed inhibition of cancer cell line DOV13. One of the most potent inhibitors **2aa** showed moderate to excellent selectivity against a range of kinases. The selectivity against AGC family kinases, especially PKA, is poor. The co-crystal structure with PKA will guide the structure-based inhibitor design. Effort to develop more selective inhibitors for AKT is underway and the results will be reported in due course.

References and notes

- Scheid, M. P.; Woodgett, J. R. *FEBS Lett.* **2003**, *546*, 108.
- Bellacosa, A.; Testa, J. R.; Moore, R.; Larue, L. *Cancer Biol. Ther.* **2004**, *3*, 268.
- Cheng, J. Q.; Lindsley, C. W.; Cheng, G. Z.; Yang, H.; Nicosia, S. V. *Oncogene* **2005**, *24*, 7482.
- Kumar, C. C.; Madison, V. *Oncogene* **2005**, *24*, 7493.
- Altomare, D. A.; Testa, J. R. *Oncogene* **2005**, *24*, 7455.
- Nakatani, K.; Thompson, D. A.; Barthel, A.; Sakaue, H.; Liu, W.; Weigel, R. J.; Roth, R. A. *J. Biol. Chem.* **1999**, *274*, 21528.

7. Stahl, J. M.; Sharma, A.; Cheung, M.; Zimmerman, M.; Cheng, J. Q.; Bosenberg, M. W.; Kester, M.; Sandirasegarane, L.; Robertson, G. P. *Cancer Res.* **2004**, *64*, 7002.
8. Li, Q.; Zhu, G. D. *Curr. Top. Med. Chem.* **2002**, *2*, 939.
9. Machajewski, T.; Lin, X.; Jefferson, A. B.; Gao, Z. *Annu. Rep. Med. Chem.* **2005**, *40*, 263.
10. Hanks, S. K.; Hunter, T. *FASEB J.* **1995**, *9*, 576.
11. Li, Q. W.; Keith, W.; Thomas, S.; Zhu, G.; Packard, G.; Fisher, J.; Li, T.; Gong, J.; Dinges, J.; Song, X.; Abrams, J.; Luo, Y.; Johnson, E.; Shi, Y.; Liu, X.; Klinghofer, V.; Des Jong, R.; Oltersdorf, T.; Stoll, V.; Jakob, C.; Rosenberg, S.; Giranda, V. *Bioorg. Med. Chem. Lett.* **2006**, *16*, 2000.
12. Li, Q.; Li, T.; Zhu, G. D.; Gong, J.; Claibone, A.; Dalton, C.; Luo, Y.; Johnson, E. F.; Shi, Y.; Liu, X.; Klinghofer, V.; Bauch, J. L.; Marsh, K. C.; Bouska, J. J.; Arries, S.; Jong, R. D.; Oltersdorf, T.; Stoll, V. S.; Jakob, C. G.; Rosenberg, S. H.; Giranda, V. L. *Bioorg. Med. Chem. Lett.* **2006**, *16*, 1679.
13. Collins, I.; Caldwell, J.; Fonseca, T.; Donald, A.; Bave-tsias, V.; Hunter, L. J.; Garrett, M. D.; Rowlands, M. G.; Aherne, G. W.; Davies, T. G.; Berdini, V.; Woodhead, S. J.; Davis, D.; Seavers, L. C.; Wyatt, P. G.; Workman, P.; McDonald, E. *Bioorg. Med. Chem.* **2006**, *14*, 1255.
14. Breitenlechner, C. B.; Friebe, W. G.; Brunet, E.; Werner, G.; Gaul, K.; Thomas, U.; Kunkele, K. P.; Schafer, W.; Gassel, M.; Bossemeyer, D.; Huber, R.; Engh, R. A.; Masjost, B. *J. Med. Chem.* **2005**, *48*, 163.
15. Lindsley, C. W.; Zhao, Z.; Leister, W. H.; Robinson, R. G.; Barnett, S. F.; Defeo-Jones, D.; Jones, R. E.; Hartman, G. D.; Huff, J. R.; Huber, H. E.; Duggan, M. E. *Bioorg. Med. Chem. Lett.* **2005**, *15*, 761.
16. The deposition number is 2GU8 with the Protein Data Bank (PDB) database.